

Non-Invasive Assessment of Sediment Accumulation Using Muography: A Pilot Run at the Shanghai Outer Ring Tunnel

Kim Siang Khaw,^{1, a)} Siew Yan Hoh,¹ Tianqi Hu,¹ Xingyun Huang,¹ Jun Kai Ng,¹ Yusuke Takeuchi,¹ Min Yang Tan,¹ Jiangtao Wang,¹ Yinghe Wang,¹ Guan Ming Wong,¹ Mengjie Wu,¹ Ning Yan,^{1, b)} Yonghao Zeng,¹ Min Chen,² Shunxi Gao,² Lei Li,² Yujin Shi,² Jie Tan,² Qinghua Wang,² Siping Zeng,² Shibin Yao,³ Yufu Zhang,⁴ Gongliang Chen,⁵ Houwang Wang,⁵ Jinxin Lin,⁶ and Qing Zhan⁶

¹⁾*Tsung-Dao Lee Institute and School of Physics and Astronomy, Shanghai Jiao Tong University, Shanghai 201210, China*

²⁾*Shanghai Geological Engineering Exploration (Group) Co., Ltd, Shanghai 200092, China*

³⁾*Shanghai Municipal Bureau of Planning and Natural Resources, Shanghai 200001, China*

⁴⁾*Shanghai Chengtou Highway Group (Group) Co., Ltd, Shanghai 200335, China*

⁵⁾*Shanghai Surveying and Mapping Institute, Shanghai 200063, China*

⁶⁾*Shanghai Institute of Natural Resources Survey and Utilization, Shanghai 200040, China*

(Dated: 2 April 2025)

This study demonstrates the application of cosmic-ray muography as a non-invasive method to assess sediment accumulation and tidal influences in the Shanghai Outer Ring Tunnel, an immersed tube tunnel beneath the Huangpu River in Shanghai, China. A portable, dual-layer plastic scintillator detector was deployed to conduct muon flux scans along the tunnel's length and to continuously monitor muon flux to study tidal effects. Geant4 simulations validated the correlation between muon attenuation and overburden thickness, incorporating sediment, water, and concrete layers. Key findings revealed an 11% reduction in muon flux per meter of tidal water level increase, demonstrating a strong anti-correlation (correlation coefficient: -0.8) with tidal cycles. The results align with geotechnical data and simulations, especially in the region of interest, confirming muography's sensitivity to sediment dynamics. This work establishes muography as a robust tool for long-term, real-time monitoring of submerged infrastructure, offering significant advantages over conventional invasive techniques. The study underscores the potential for integrating muography into civil engineering practices to enhance safety and operational resilience in tidal environments.

^{a)}Electronic mail: kimsiang84@sjtu.edu.cn

^{b)}Present address: Department of Physics, Brown University, Rhode Island 02912, USA

I. MOTIVATION

Urban infrastructure, such as cross-river tunnels, plays a vital role in maintaining the functionality and connectivity of modern cities. In megacities like Shanghai, where rapid development coexists with aging subterranean structures, ensuring the safety and reliability of immersed tunnels has become increasingly important. These structures are subject to continuous geotechnical changes due to sediment accumulation, groundwater dynamics, and tidal influences—factors that can compromise structural integrity over time.

However, monitoring the health status of immersed tube tunnels remains a significant engineering challenge. Traditional geotechnical techniques, such as borehole drilling, sonar scanning, or multibeam echo sounder systems¹ (MBES), are either invasive, limited in resolution, or incapable of providing continuous temporal coverage. They may also require deploying personnel into hazardous environments or interrupting tunnel operations and river traffic—limitations that hinder effective long-term risk assessment.

Moreover, the sediment dynamics above cross-river tunnels are highly variable, driven by natural hydrological forces such as tidal cycles in estuarine environments like the Huangpu River. Under these conditions, minor yet cumulative overburden changes—such as uneven sediment deposition or scouring—can lead to differential settlements and ultimately impact tunnel stability. Addressing this monitoring gap requires innovative, passive, and non-disruptive techniques that can be deployed in urban settings without disrupting ongoing operations.

Muography² offers a promising solution to this problem. By utilizing naturally occurring cosmic-ray muons to probe variations in material density, this technique enables the internal imaging of large-scale structures without the need for artificial radiation or excavation. Muons are highly penetrating particles capable of traversing hundreds of meters of rock and soil. As they pass through a material, their attenuation depends on the integrated density along their paths. By measuring the muon flux and comparing it to open-sky expectations, we can infer changes in overburden—such as sediment accumulation—with high precision. A pioneering effort for muography was done by Eric George in 1955 to measure the ice thickness above a tunnel in Australia³.

While muography has been effectively employed in archaeological investigations^{4,5}, volcanic imaging⁶, mine exploration⁷, and tidal-wave and tsunami monitoring^{8,9}, its potential

for monitoring urban infrastructure—particularly in submerged and sediment-prone environments—remains largely untapped. Recent studies have demonstrated its applicability to railway and metro tunnels for detecting hidden shafts¹⁰ and voids^{11,12}; however, few investigations have examined its use in tracking temporal changes in the overburden due to natural hydrodynamic processes.

In this study, we report a pilot run of muography application to a cross-river immersed tube tunnel: the Shanghai Outer Ring Tunnel. This tunnel is a key segment of the Shanghai S20 expressway running beneath the Huangpu River. We deployed a portable, field-ready muon detection system in two complementary modes:

- a spatial scan along the tunnel axis to map variations in overburden thickness, and
- a fixed-point continuous monitoring system to examine the relationship between muon flux and tidal effects.

Supporting Geant4 simulations were conducted to validate the system’s sensitivity to density changes. Our results show that muography can detect both spatial and temporal overburden variations in a live tunnel environment, establishing its feasibility as a non-invasive tool for infrastructure health monitoring in dynamic urban settings. This pilot study provides a foundation for the future deployment of muon detectors as part of smart urban sensing networks for resilient and data-driven infrastructure management.

This article is systematically structured as follows: Section II offers an introduction to the Shanghai Outer Ring Tunnel. Section III elaborates on the muon detector and the data acquisition system utilized during the field trials. Section IV outlines the measurements conducted during these trials. An analysis of the data and interpretation of the results are addressed in Section V. Furthermore, a discussion regarding the potential applications of muography in cross-river tunnels is provided in Section VI, culminating in Section VII, which concludes the study.

II. SHANGHAI OUTER RING TUNNEL

The Shanghai Outer Ring Tunnel, as depicted in Fig. 1, is an essential part of the Shanghai S20 expressway, facilitating vehicle travel between the Pudong (east of Huangpu River) and Puxi (west of Huangpu River) districts of Shanghai under the Huangpu River. As shown

in Fig. 2, this tunnel features a 43 m wide, 9.55 m high reinforced rectangular structure. It spans 2,882 m in length and consists of three tubes that support eight lanes, along with two service galleries between the tubes dedicated to rescue operations and cabling. The submerged section of the tunnel spans a length of 736 meters and is composed of seven segments, E1 through E7. E1 begins on the western side of the tunnel. Segment E2 is located at the slopes of the tunnel site, while segments E3 to E7 gradually rise toward the eastern side.

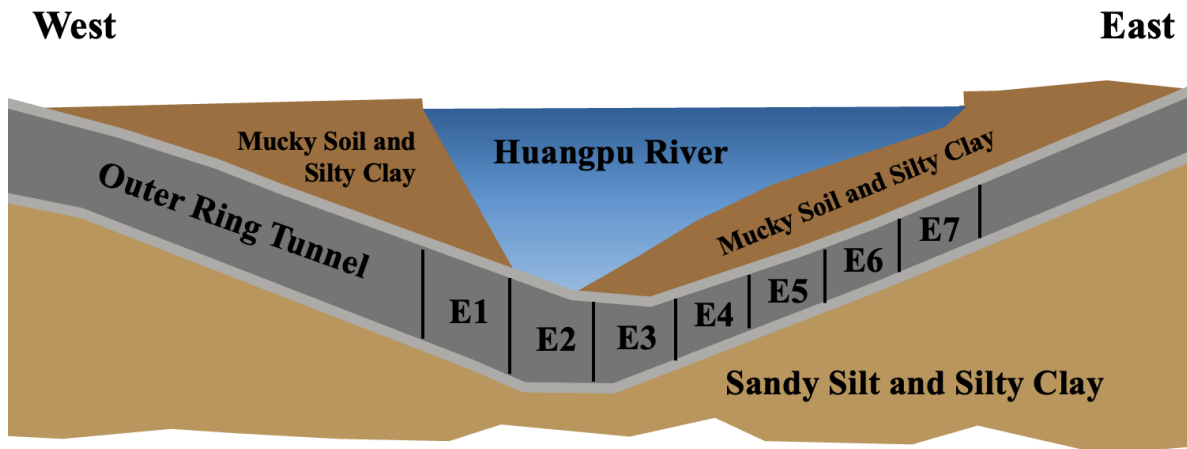


FIG. 1. A simplified geological profile for the outer ring tunnel at Huangpu river¹³.

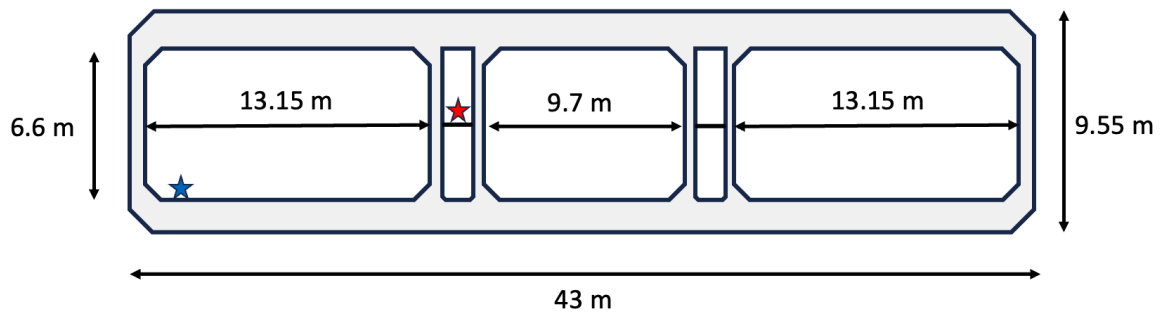


FIG. 2. Transverse cross-section view of the Shanghai Outer Ring Tunnel. The blue star indicates the detector location for spatial tunnel scan, and the red star indicates the detector installation location (left service gallery) for continuous muon flux monitoring.

Figure 1 illustrates a simplified geotechnical and geomorphic profile along the tunnel's alignment¹³⁻¹⁵. The terrain at the tunnel site slopes sharply to the west and gently to the

east. Beneath the river lies a deep trough reaching a depth of 23.6 m, forming an asymmetrical V-shaped riverbed. Geologically, the tunnel is situated within soil strata beneath the riverbed, comprised of sedimentary deposits commonly found in riverine environments. These overburdens consist of naturally deposited sediments such as gray sandy silt, mucky silty clay, gray mucky silty clay, muck clay, and predominantly gray mealy sand¹³, which have formed over time through weathering, erosion, and sedimentation. These sediments primarily consist of fine-grained particles displaying density variations that are influenced by factors such as organic content, compaction, and water saturation, typically ranging from 1.5 to 2.0 g/cm³. These materials vary in composition and properties: gray sandy silt and gray mealy sand are granular with moderate permeability, facilitating drainage, while mucky silty clay and gray mucky silty clay contain higher clay content, leading to lower permeability and increased cohesion. Muck clay, composed of fine-grained organic-rich material, has high plasticity and water retention, potentially affecting tunnel stability and settlement behavior. Since its commissioning in 2003, the tunnel has shown signs of differential settlement caused by river flow, particularly at segment joints in the submerged sections E4-E6, leading to water leakage into the tunnel. Moreover, the sediment thickness at the E5-E6 sections is now several meters above the design value, causing increased stress on structural stability.

Additionally, tidal influences from the Huangpu River lead to periodic changes in water levels and flow velocities, complicating the surrounding environment. These dynamic conditions, combined with the river’s freshwater properties, create an environment that is both challenging and stimulating for structural monitoring and analysis. The interaction between the tunnel, sediments, and tidal forces emphasizes the need for advanced techniques to assess and maintain the tunnel’s structural integrity time.

III. MUON DETECTOR DESIGN AND DATA ACQUISITION SYSTEM

The muon detection system design emphasizes efficient field deployment to withstand the challenging conditions of construction sites during the maintenance period from March 2024 to March 2025. The system must be robust, easy to assemble and operate, and have low power consumption. A dual-layer detector made up of two HDN-S2 plastic scintillators from GaoNengKeDi is used to measure the muon flux after passing through the overburden above the outer ring tunnel. Each plastic scintillator has a dimension of $80 \times 20 \times 2 \text{ cm}^3$,

providing a total active area of $1,600 \text{ cm}^2$. These two scintillators are vertically spaced 10 cm apart and held in position by a 3D-printed support structure. This resulted in an acceptance angle of 164 degrees along the long axis and 126 degrees along the short axis. To maximize light collection, the scintillators are coupled with light guides matched to the NVN N4021 photomultiplier tubes¹⁶ (PMTs). A high-voltage module is also built into the PMT, enabling the detector to be operated using a commercially available 12 V low-voltage portable power unit.

Two different versions of the data acquisition system (DAQ) were used during the field trials. For the spatial scan measurements used in the overburden profile study, the signals from the PMTs were digitized by the DRS4 waveform digitizer¹⁷ connected to a laptop computer. A schematic of the DAQ system is depicted in Fig. 3. A double coincidence trigger was used to record the muon events. The threshold was set at 0.1 V, where the most probable value (MPV) for the muon energy deposition distribution is around 0.15 V. A typical muon event's double coincidence waveforms are shown in Fig. 4.

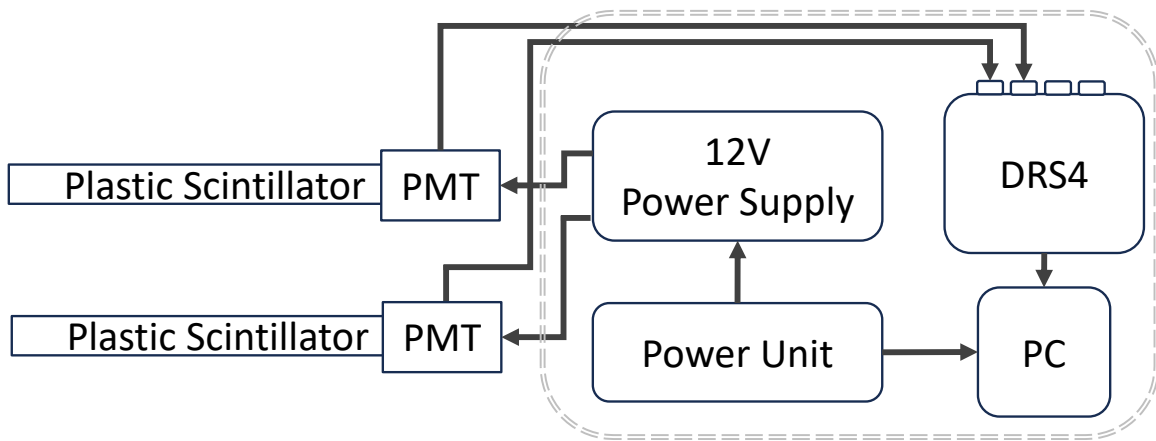


FIG. 3. The schematic of the muon detection system used for tunnel spatial scan measurements. The dashed outline highlights the DAQ system used to process signals from the plastic scintillators.

On the other hand, for long-term monitoring of muon flux variations due to tidal effects, a custom-built coincidence logic circuit on a printed circuit board (PCB) is utilized in conjunction with an Arduino UNO v3 and a Raspberry Pi 4, as shown in Fig. 5. This configuration is optimized to reduce power consumption (by replacing the laptop with a Raspberry Pi) for efficient and sustained operation. Specifically, this system removes the necessity for an

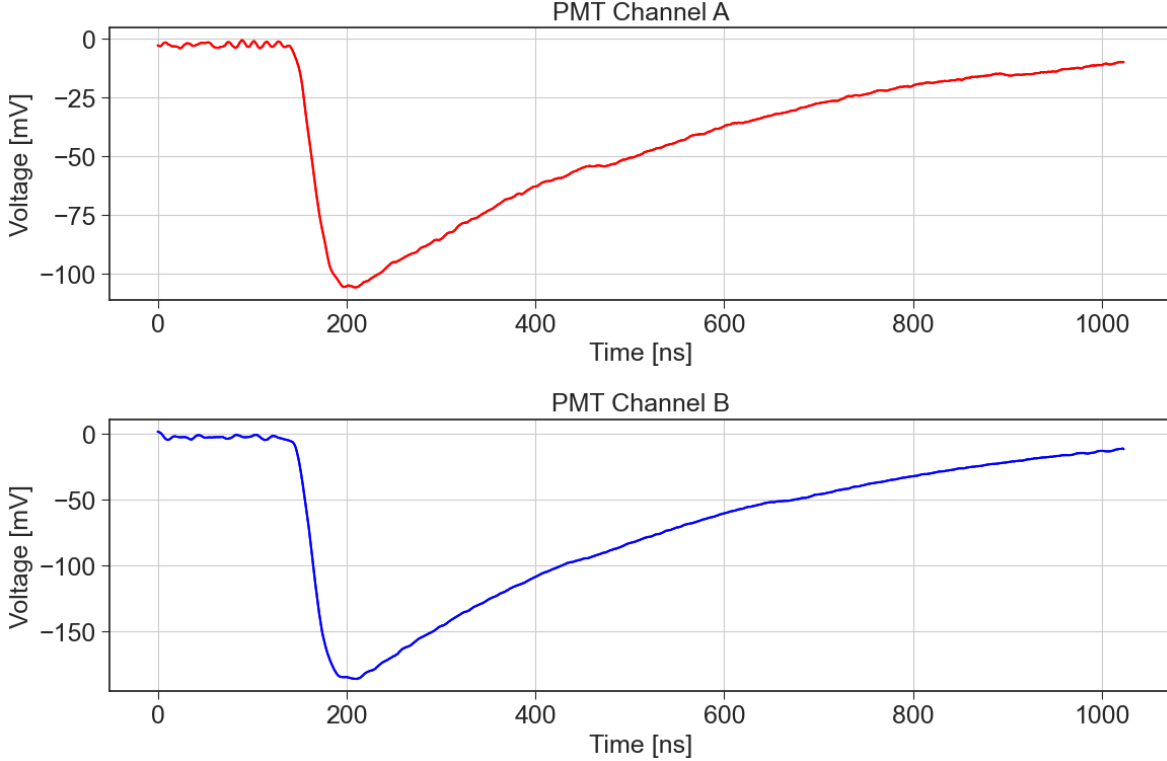


FIG. 4. A typical event where both PMTs observed a double coincidence signal from the muon.

on-site power source, which is often unavailable in construction or remote areas, thereby enhancing portability and suitability for long-term monitoring. Both systems are powered by a portable outdoor lithium power unit (GNV-ZC1100) with a 1 kWh capacity, capable of delivering 1 kW, and weighing 14.3 kg. Prior to the deployment, we have calibrated both detectors and the DAQ system to ensure they provide consistent results in terms of the measured muon flux.

IV. SHANGHAI OUTER RING TUNNEL FIELD TRIAL

A. Muon Flux Spatial Scan in the Tunnel

From December 26 to 27, 2024, a muon flux scanning operation of the Shanghai Outer Ring Tunnel was carried out using the mobile muon detection system, as illustrated in Fig. 6. The operation commenced at E7 on the east side and adhered to a strict measurement protocol to ensure accuracy and consistency. At the E7 entrance, the lateral position of the detection system was consistently maintained at approximately 2.3 m from the left tunnel

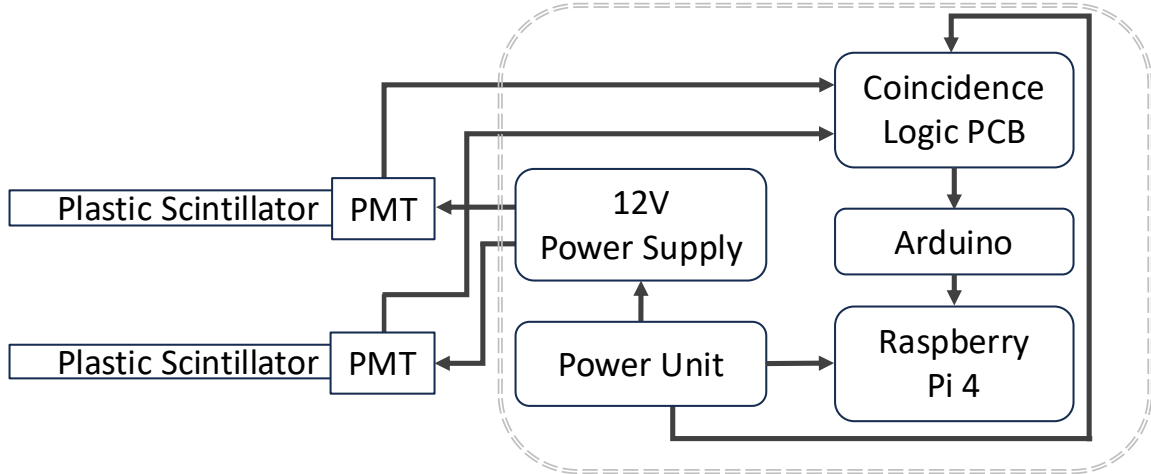


FIG. 5. The schematic of the muon detection system used for the continuous tidal wave monitoring. The dashed outline highlights the DAQ system used to process signals from the plastic scintillators.

wall (indicated as a blue star in Fig. 2) throughout the measurement campaign. Using a laser-based distance measuring tool, measurements were taken every 10 minutes, spaced 50 m apart along the tunnel’s length. Since the tunnel was under maintenance during the measurement period, on-site construction activities and occasional large truck movements occupied the whole highway. In such instances, ongoing measurements were discarded and restarted once conditions improved. The scanning concluded at E1, covering approximately 5 hours and yielding 15 measurement points within the tunnel. Additionally, open-sky measurements were conducted to calibrate the detector and establish the baseline muon flux, employing the same detection system placed outside the tunnel during the measurement process.

B. Continuous Muon Flux Monitoring

To study the influence of tidal effects on muon flux measurement, an additional muon detection system, as shown in Fig. 7, was deployed to continuously monitor the muon flux at the deepest location in the tunnel, segment E2. Above the tunnel, the water column is about 20 m. This detector was situated in the left service gallery of the tunnel (red star in Fig. 2) and monitored the muon flux for 1.5 days from January 15 to 17, 2025. This configuration significantly reduced power consumption to approximately 20 watts, allowing



FIG. 6. A photograph of the muon detection system measuring muon flux at a location during the muon flux spatial scan campaign in the Shanghai Outer Ring Tunnel.

the muon detection system to operate continuously for over 36 hours.

C. The Outer Ring Tunnel Simulation

To validate the measurement results from the scanning operation, a simplified model of the Shanghai Outer Ring Tunnel and its surroundings was constructed. The model divides the $740 \times 50 \text{ m}^2$ area encapsulating the tunnel into 37 equal-size discrete bins, each with an area of $20 \times 50 \text{ m}^2$, and varying height depending on the material budget, as shown in Fig. 8. The material budget for the tunnel, including water, sediment, and concrete, is based on the technical drawing of the tunnel and the MBES scan conducted in 2024. The interaction of muons with the material in the model was simulated using the Geant4-based¹⁸ `musrSim`¹⁹ package.

The water density of 1.02 g/cm^3 is selected to reflect the freshwater characteristics and

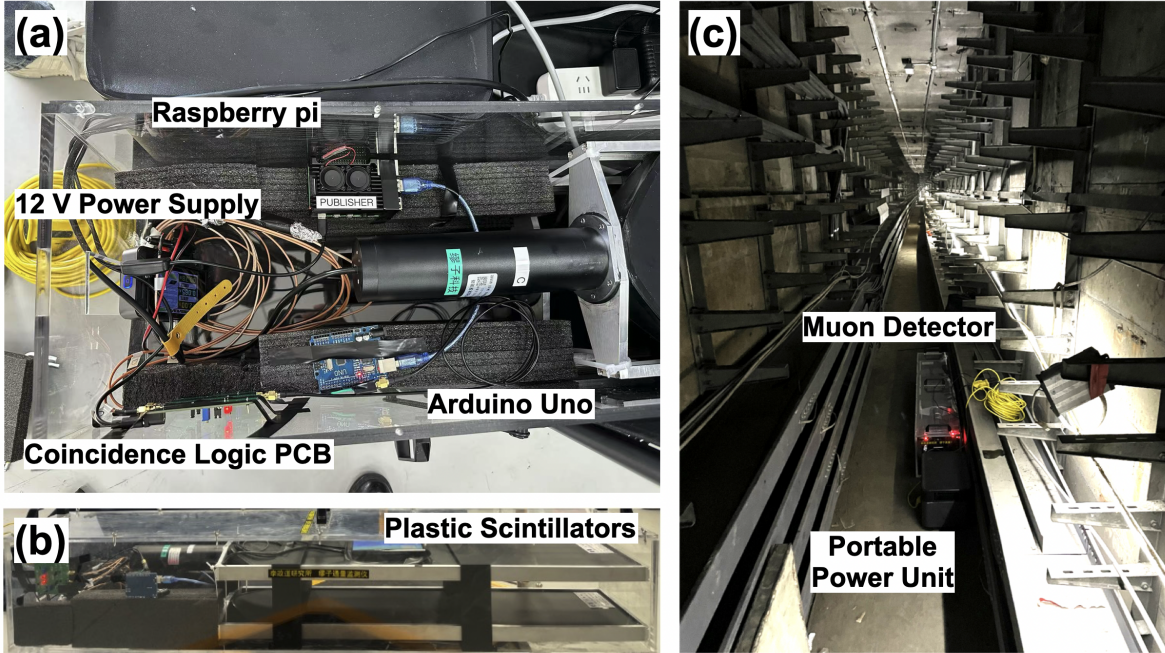


FIG. 7. (a) DAQ components consist of low-cost electronics, including a Raspberry Pi, Arduino Uno, coincidence logic PCB, and power supply; (b) The dual-layered muon detector is housed in an acrylic enclosure for protection; (c) Installation of the muon detection system on the second floor of the Shanghai Outer Ring Tunnel.

typical temperature range of the Huangpu River. Water density usually fluctuates between 0.995 and 1.05 g/cm^3 , depending on temperature variations from 15 to $30 \text{ }^\circ\text{C}$ and local conditions. While suspended solids and dissolved particles can slightly raise water density, their overall impact remains minimal compared to other environmental factors. On the other hand, the collective sediment density of 1.8 g/cm^3 represents the less compacted, water-saturated quality of the gray mealy sand used to simulate the sediment element.

The third layer of the overburden profile consists of the top tunnel wall, which is made of concrete with a thickness of 2 m and a density of 2.5 g/cm^3 . Beneath the top tunnel wall, there is an additional 6 m of air column, representing the height of the tunnel. Subsequently, a series of muon detectors are positioned at the center of each bin to measure the expected muon flux.

Tidal effects can alter the height of the water column above the tunnel, temporarily changing the overburden thickness, thus affecting the muon flux. Although this dynamic effect is not considered in this simulation, it can be estimated using the tidal height data

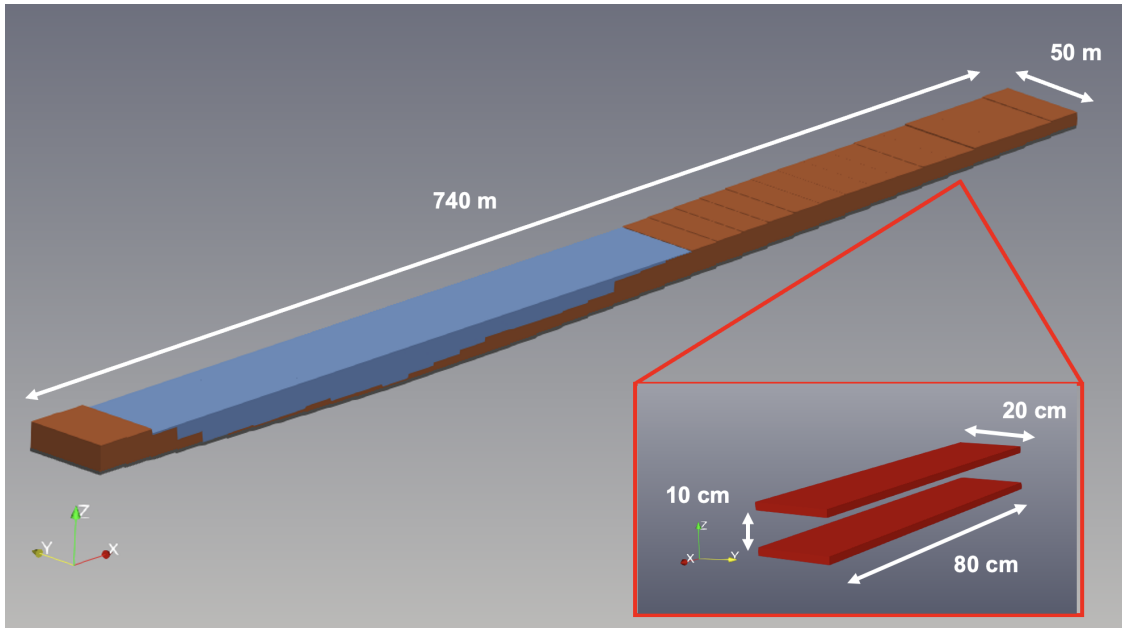


FIG. 8. The simulated tunnel model, measuring 740 m in length and 50 m in width, consists of 37 different segmented overburden profiles made up of water (blue), sediment (brown), and concrete (black). The dual-layered detector is indicated in red box.

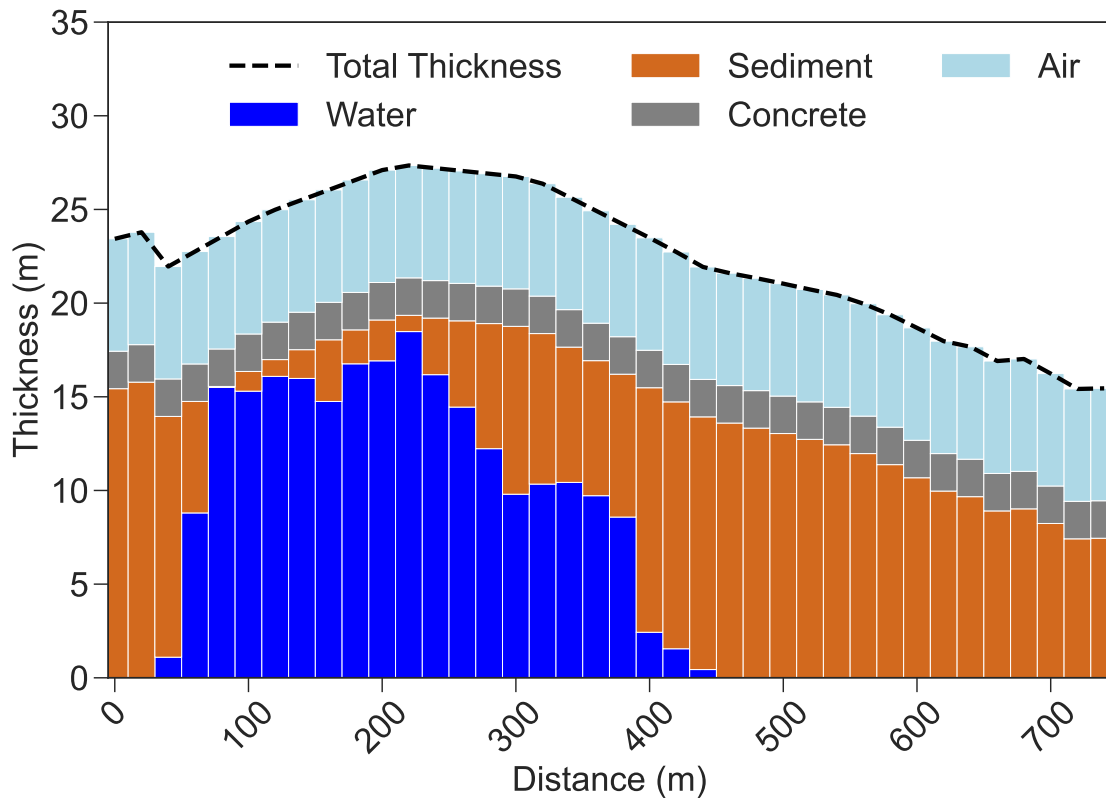


FIG. 9. Material budget above the tunnel along the tunnel axis in the Geant4 simulation.

during the measurement period and the continuous muon flux monitoring data.

To simulate cosmic-ray muon events with realistic angular and energy distributions, the EcoMug generator²⁰ is used to generate cosmic-ray muons from a sky-plane, emitting at a rate of 129 Hz/m^2 , corresponding to an exposure of about 1 minute. The attenuation of muons due to overburden above the tunnel is studied by positioning a plane source of size $800 \times 50 \text{ m}^2$ at a height of 14 m above the tunnel.

V. DATA ANALYSIS AND INTERPRETATION

A. Temporal Correlation with Tidal Effects

In order to accurately interpret the results of the muon flux spatial scan, we first conducted an analysis of the temporal correlation between muon flux and tidal effects. The variation in tidal height influences the thickness of the water layer, which, in turn, significantly affects the muon absorption rate by altering the overall overburden budget. To assess this relationship, concurrent measurements of tidal height obtained from the Wusongkou tidal gauge station, situated approximately 3 km north of the Shanghai Outer Ring Tunnel (see Fig. 10), were utilized to analyze the recorded muon flux during specific dates and time intervals.

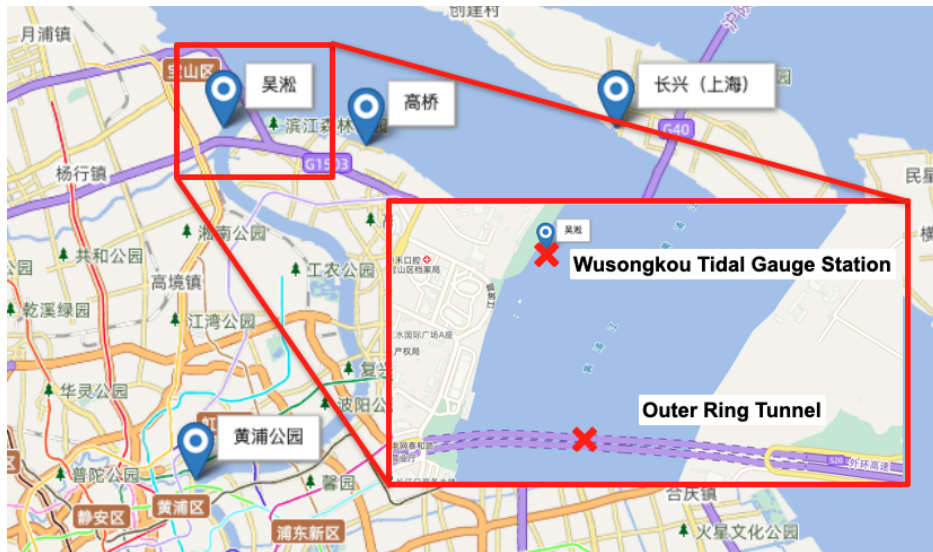


FIG. 10. The location of the Wusongkou tidal gauge station ($31^\circ 22' 56.2'' \text{ N}$, $121^\circ 30' 18.6'' \text{ E}$) and the Outer Ring Tunnel ($31^\circ 22' 37.6'' \text{ N}$, $121^\circ 30' 23.1'' \text{ E}$).

Figure 11 illustrates the correlation between muon counts (recorded every 10 minutes) and variations in astronomical tide height (ATH) measured at the Wusongkou tidal gauge station. The data clearly demonstrate periodic fluctuations in muon flux that correspond to the tidal cycles, with the muon flux decreasing by approximately 11% for each meter increase in water level, consistent with theoretical expectations. The plot highlights how muon flux decreases or increases in response to rising or falling tidal heights, respectively. The measured correlation between muon flux and ATH revealed a strong anti-correlation relationship, as shown in Fig. 12. Interestingly, this pattern mirrors observations from the Tokyo Bay TS-HKMSDD experiment⁹, which detected periodic muon flux oscillations corresponding to tidal cycles. This observation underscores the importance of considering tidal effects in future efforts to monitor sediment thickness in regions where both river water and sediment coexist.

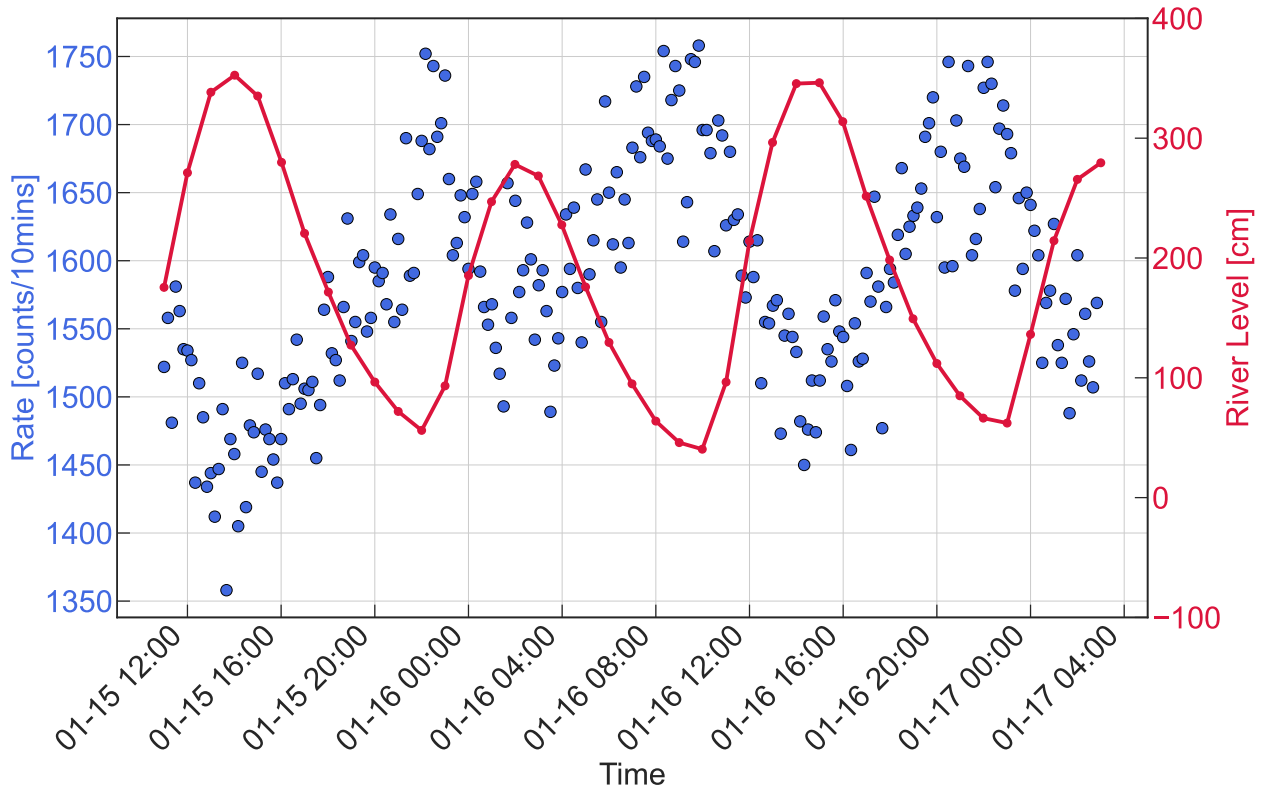


FIG. 11. Time-sequential plot of the number of muon counts collected every 10 min (dark blue dots) and the river water level (202 cm below mean sea level) measured at the Wusongkou tidal gauge station (red curve).

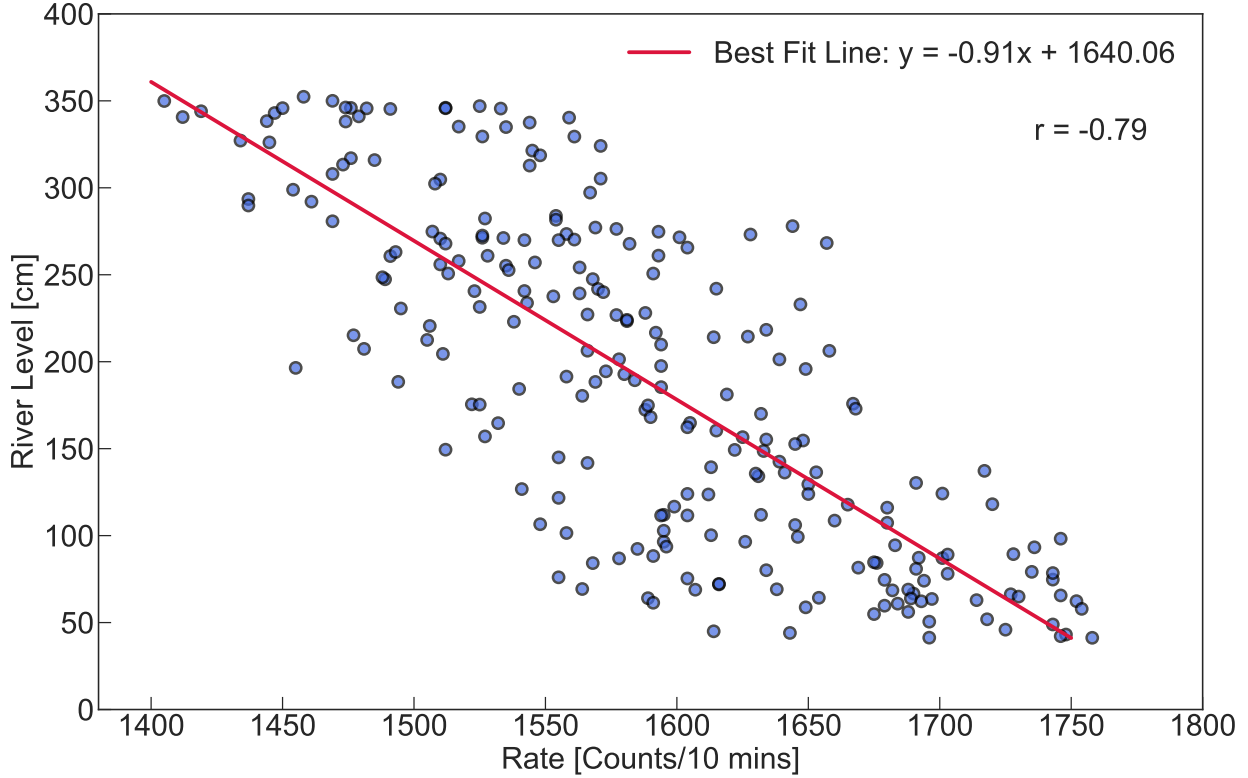


FIG. 12. A scatter plot of river water levels and measured muon flux per 10 minutes. The correlation coefficient is measured at -0.8.

B. Spatial Variation in Muon Flux

The collected muon dataset from the Spatial Scan campaign is converted into muon flux per minute and compared to the overburden profile as a function of distance, starting from the east entrance of the immersed tube tunnel at E1, as shown in Fig. 13. The spatial scan reveals systematic variations in muon flux along the tunnel that are closely correlated with changes in sediment thickness and tunnel elevation. The errors indicated on the muon flux rate are purely statistical.

Generally, the measured flux aligns closely with the simulated flux along the tunnel axis. The variation in muon flux is less pronounced compared to the overburden profile, mainly due to the detector's large acceptance angle (allowing for a broader range to be mapped) and the relatively small integrated density along the muon path, given the changing tunnel depth. Notably, the measured and expected muon flux show excellent agreement in the region dominated by sediment, which is also the region of interest (E4-E6) in this study,

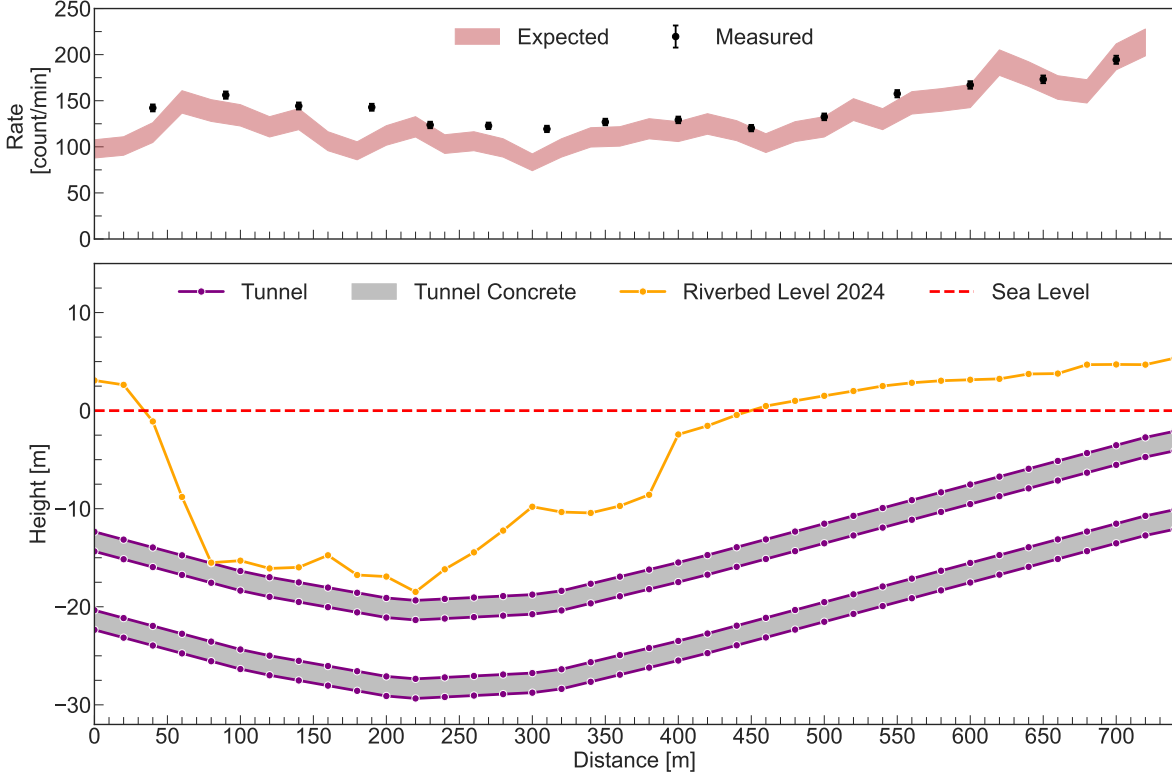


FIG. 13. Top: Measured muon flux at 15 locations along the tunnel length. Bottom: Current riverbed profile measured with MBES in 2024 along the tunnel direction.

specifically from 350 m to the right (west), whereas the measured flux is consistently higher in the area dominated by river water.

The systematic differences between the expected and measured muon flux at the deepest region of the tunnel can be attributed to various potential sources of error or approximation in the simulation and environmental conditions. One of the factors is that the measured riverbed has an uncertainty of 0.5 m and it is not represented in Fig. 13. If the actual riverbed at a single point is 0.5 m this means the expected muon flux should go up by around 5% based on the results from the tidal effect analysis. Another factor is the simplification of material properties in the simulation, such as the assumption of uniform density for both sediment and water. In reality, the densities of sediment and water can vary due to factors like organic content, compaction, and water saturation, which are not fully captured in the model. In the next step, we plan to build a more accurate model of the tunnel and its surroundings.

VI. DISCUSSION

Building on these findings, future work will focus on enhancing the precision and scope of muography for continuous structural monitoring of cross-river tunnels. Optimizing detector design and deployment locations will improve resolution, enabling more detailed tracking of sediment accumulation and structural changes. Additionally, developing an advanced algorithm to reconstruct settlement thickness variations along the tunnel’s length will provide a more comprehensive understanding of deformation patterns over time. Expanding the muon detector network to within the tunnel and to multiple tunnels beneath the Huangpu River will further establish muography as a robust tool for large-scale subsurface monitoring. These advancements will strengthen the foundation for long-term, data-driven infrastructure assessment, ensuring the reliability and safety of critical underwater structures.

VII. CONCLUSION

In conclusion, this study presents a preliminary application of muography as a robust method for monitoring sediment thickness and assessing tidal influences within the Shanghai Outer Ring Tunnel. The successful muon flux spatial scan conducted in the tunnel, coupled with long-term monitoring at a fixed site, demonstrates the method’s reliability for detecting overburden changes in complex environments. Findings show a strong alignment between measured muon flux and theoretical predictions, confirming the accuracy of Geant4 simulations in replicating observed muon attenuation in the area of interest.

More importantly, the anti-correlation observed between muon flux and tidal variations showcases the utility of muography in non-invasive tidal monitoring. This highlights the technique’s potential to track sediment accumulation and ensure long-term tunnel stability. These results not only establish a foundation for future continuous monitoring projects but also affirm muography’s effectiveness as a powerful tool in the analysis of subsurface infrastructure. As further research and application are conducted, muography may significantly contribute to the field of geophysical monitoring and the management of infrastructure integrity.

ACKNOWLEDGMENTS

We wish to express our heartfelt gratitude to Jining Chen from the Shanghai Municipality for proposing the innovative application of muography in infrastructure studies within the Shanghai region. Our special appreciation extends to Yuxin Zhang from the Shanghai Municipal Bureau of Planning and Natural Resources and Jie Zhang from Shanghai Jiao Tong University for initiating this interdisciplinary research collaboration. We sincerely thank the staff at Shanghai Tunnel Engineering Co., Ltd. for their invaluable assistance with muon flux measurements and the deployment of the long-term monitoring detectors. We would also like to extend our gratitude to the administrative staff—Shushu Li, Rongrong Zhang, Sheng Li, Jinghua Shi, Xiaoqian Jin, Xiaojun Lu, and Mengzhu Lu—at the Tsung-Dao Lee Institute, Shanghai Jiao Tong University, for their support in the startup of the TDLI Muography Group. This work was financially supported by the Tsung-Dao Lee Institute Special Research Grant for Muography Applications in Shanghai, as well as the Double First Class Start-up Fund provided by Shanghai Jiao Tong University.

REFERENCES

- ¹F. Thomas, F. A. Livio, F. Ferrario, M. Pizza, and R. Chalaturnyk, “A review of subsidence monitoring techniques in offshore environments,” *Sensors* **24** (2024), 10.3390/s24134164.
- ²L. Bonechi, R. D’Alessandro, and A. Giammanco, “Atmospheric muons as an imaging tool,” *Rev. Phys.* **5**, 100038 (2020), arXiv:1906.03934 [physics.ins-det].
- ³E. P. George, “Cosmic Rays Measure Overburden of Tunnel,” *Commonwealth Engineer* **42**, 455–457 (1955).
- ⁴L. W. Alvarez *et al.*, “Search for Hidden Chambers in the Pyramids,” *Science* **167**, 832–839 (1970).
- ⁵K. Morishima *et al.*, “Discovery of a big void in Khufu’s Pyramid by observation of cosmic-ray muons,” *Nature* **552**, 386–390 (2017), arXiv:1711.01576 [physics.ins-det].
- ⁶K. Nagamine, M. Iwasaki, K. Shimomura, and K. Ishida, “Method of probing inner structure of geophysical substance with the horizontal cosmic ray muons and possible application to volcanic eruption prediction,” *Nucl. Instrum. Meth. A* **356**, 585–595 (1995).

- ⁷G. Liu *et al.*, “Deep investigation of muography in discovering geological structures in mineral exploration: a case study of Zaozigou gold mine,” *Geophys. J. Int.* **237**, 588–603 (2024).
- ⁸H. Tanaka, C. Bozza, R. Coniglione, J. Gluyas, S. Steigerwald, M. Holma, P. Kuusiniemi, G. Leone, H. Mori, J. Matsushima, S. Paling, D. Lo Presti, T. Kin, O. Kamoshida, M. Aichi, L. Oláh, K. Sumiya, L. Thompson, Y. Yokota, and M. Satoh, “First results of undersea muography with the tokyo-bay seafloor hyper-kilometric submarine deep detector magma-hkmsdd collaboration,” (2021).
- ⁹H. Tanaka, M. Aichi, S. Balogh, C. Bozza, R. Coniglione, J. Gluyas, N. Hayashi, M. Holma, J. Joutsenvaara, O. Kamoshida, Y. Kato, T. Kin, P. Kuusiniemi, G. Leone, D. Lo Presti, J. Matsushima, H. Miyamoto, H. Mori, Y. Nomura, and D. Varga, “Periodic sea-level oscillation in tokyo bay detected with the tokyo-bay seafloor hyper-kilometric submarine deep detector (ts-hkmsdd),” *Scientific Reports* **12**, 6097 (2022).
- ¹⁰L. Thompson, J. Stowell, S. Fargher, C. Steer, K. Loughney, E. O’Sullivan, J. Gluyas, S. Blaney, and R. Pidcock, “Muon tomography for railway tunnel imaging,” *Physical Review Research* **2** (2020), 10.1103/PhysRevResearch.2.023017, cited by: 35; All Open Access, Gold Open Access, Green Open Access.
- ¹¹X. Mao, Z. Li, S. Dong, J. Li, J. Zhang, J. Pang, Y. Cheng, B. Liao, X. Ouyang, and R. Han, “Muon radiography experiments on the subway overburden structure detection,” *Nuclear Instruments and Methods in Physics Research Section A: Accelerators, Spectrometers, Detectors and Associated Equipment* **1055**, 168391 (2023).
- ¹²R. Han, Q. Yu, Z. Li, J. Li, Y. Cheng, B. Liao, L. Jiang, S. Ni, Z. Yi, T. Liu, and Z. Wang, “Cosmic muon flux measurement and tunnel overburden structure imaging,” *Journal of Instrumentation* **15**, P06019 (2020).
- ¹³S. Wang, X. Zhang, and Y. Bai, “Comparative study on foundation treatment methods of immersed tunnels in china,” *Frontiers of Structural and Civil Engineering* **14** (2019), 10.1007/s11709-019-0575-x.
- ¹⁴L. Q. Zhu Jiexiang, Chen Bin and B. Yun, “Outline of key construction techniques used in shanghai outer loop pipe-sinking tunnel,” *Geotechnical Engineering World* **8**, 2–5 (2003).
- ¹⁵J. Jacob, *Optimization of Design and Monitoring of Immersed Tunnels*, Master’s thesis, Delft University of Technology (2022).
- ¹⁶North Night Vision Technology (Nanjing) Research Institute Co., Ltd. (NVN):

<http://yskijnj.com/product/detail-35.html>.

- ¹⁷S. Ritt, R. Dinapoli, and U. Hartmann, “Application of the DRS chip for fast waveform digitizing,” *Nucl. Instrum. Meth. A* **623**, 486–488 (2010).
- ¹⁸S. Agostinelli *et al.* (GEANT4), “GEANT4 - A Simulation Toolkit,” *Nucl. Instrum. Meth. A* **506**, 250–303 (2003).
- ¹⁹K. Sedlak, R. Scheuermann, T. Shiroka, A. Stoykov, A. R. Raselli, and A. Amato, “Musrsim and musrsimana - simulation tools for μ sr instruments,” *Physics Procedia* **30**, 61–64 (2012).
- ²⁰D. Pagano, G. Bonomi, A. Donzella, A. Zenoni, G. Zumerle, and N. Zurlo, “Ecomug: An efficient cosmic muon generator for cosmic-ray muon applications,” *Nuclear Instruments and Methods in Physics Research Section A: Accelerators, Spectrometers, Detectors and Associated Equipment* **1014**, 165732 (2021).